Available online at www.sciencedirect.com
ScienceDirect
Catalysis Today 131 (2008) 457–463
CATALYSIS TODAY
www.elsevier.com/locate/cattod

Design of a novel bifunctional catalyst $IrFe/Al_2O_3$ for preferential CO oxidation

Wansheng Zhang [a,b], Aiqin Wang [a], Lin Li [a], Xiaodong Wang [a], Tao Zhang [a,*]

[a] State Key Laboratory of Catalysis, Dalian Institute of Chemical Physics, Chinese Academy of Sciences, Dalian 116023, China
[b] Graduate School of the Chinese Academy of Sciences, Beijing 100049, China

Available online 26 November 2007

Abstract

In this study, a novel bifunctional catalyst $IrFe/Al_2O_3$, which is very active and selective for preferential oxidation of CO under H_2-rich atmosphere, has been developed. When the molar ratio of Fe/Ir was 5/1, the $IrFe/Al_2O_3$ catalyst performed best, with CO conversion of 68% and oxygen selectivity towards CO_2 formation of 86.8% attained at 100 °C. It has also been found that the impregnation sequence of Ir and Fe species on the Al_2O_3 support had a remarkable effect on the catalytic performance; the activity decreased following the order of $IrFe/Al_2O_3$ > co-$IrFe/Al_2O_3$ > $FeIr/Al_2O_3$. The three catalysts were characterized by XRD, H_2-TPR, FT-IR and microcalorimetry. The results demonstrated that when Ir was supported on the pre-formed Fe/Al_2O_3, the resulting structure ($IrFe/Al_2O_3$) allowed more metallic Ir sites exposed on the surface and accessible for CO adsorption, while did not interfere with the O_2 activation on the FeO_x species. Thus, a bifunctional catalytic mechanism has been proposed where CO adsorbed on Ir sites and O_2 adsorbed on FeO_x sites; the reaction may take place at the interface of Ir and FeO_x or via a spill-over process.

Keywords: CO oxidation; PROX; Ir-Fe catalyst; Iridium; Microcalorimetry

1. Introduction

Proton exchange membrane fuel cells (PEMFC) are becoming an increasingly attractive technology for electrical power generation [1,2]. The hydrogen from hydrocarbon fuels is generally obtained via the partial oxidation and the steam reforming processes. Since carbon monoxide is always present in the gas mixtures (0.5–1%) produced from these hydrocarbon fuels, it must be removed to a level of less than 20 ppm in order to avoid the poisoning of platinum electro-catalyst in the anode of fuel cells [3]. Preferential oxidation (PROX) of carbon monoxide by oxygen in excess hydrogen atmosphere is considered to be a promising method to reduce the content of carbon monoxide to an acceptant level for use in PEMFC [4]. Supported platinum-based catalysts have particularly been considered for the elimination of carbon monoxide in hydrogen-rich streams [5]. Subsequently, other supported noble metal catalysts (Pd, Ru, and Rh) have also been tested for PROX [6,7]. Generally, oxidation of CO on these noble-metal-based catalysts is a multi-step process obeying a single-site competitive Langmuir–Hinshelwood mechanism, where CO, H_2 and O_2 compete for adsorption on noble metal surface. At low temperatures, O_2 can hardly be adsorbed on the surface covered with strongly adsorbed CO layer leading to low CO conversions. Only at high temperatures there are some adsorbed CO species escaping from the surface, leaving space for O_2 adsorption and reaction with the neighboring adsorbed CO to produce CO_2. However, at this high temperature, another unexpected reaction of H_2 oxidation becomes more competitive. In contrast with the extensive investigations on the Pt-based catalysts, supported Ir catalysts received only little attention for this reaction. Okumura et al. prepared a series of Ir catalysts by deposition precipitation (DP) method and found that Ir/TiO_2 was much more highly active than on other metal oxides supports for CO oxidation at low temperature [8]. However, losing of the Ir component during the DP process is inevitable. Mariño et al. [9] reported iridium supported on ceria-zirconia prepared by impregnation in an ultrasonic bath using an acetone solution of expensive precursor $Ir[CH(-COCH_3)_2]_3$ for the PROX. But the CO conversion and selectivity of O_2 towards CO_2 formation was not very high.

* Corresponding author. Tel.: +86 411 84379015; fax: +86 411 94691570.
E-mail address: taozhang@dicp.ac.cn (T. Zhang).

0920-5861/$ – see front matter © 2007 Elsevier B.V. All rights reserved.
doi:10.1016/j.cattod.2007.10.058

Recently, highly dispersed gold particles supported on single or composite oxides, have been proved to be active for PROX in particular at low temperatures [10]. The reducible metal oxide supports can provide active oxygen for reaction through direct adsorbing O_2 or transporting O_2 as a tunnel. Similar to the strategy of O_2 activation on the reducible metal oxides on the Au/MO_x, a series of Pt promoted with reducible oxide or second metal catalysts supported over various oxides, zeolites or activated carbon, including Pt-Ru [11], Pt-Fe [12–15], Pt-Co [16], Pt-Ce [17], Pt-Sn [18,19] and Pt-Ni [20] have been proposed as promising choices for PROX. Such bimetallic catalysts all behaved better performances than the corresponding monometallic ones due to the synergistic effect. The main function of the promoter 3d transition metal oxide was supposed to tune up the Pt electronic properties so that O_2 can be adsorbed on Pt sites or on metal oxide sites [11–20]. In the present work, we designed a novel and efficient catalyst system $IrFe/Al_2O_3$ which was highly active and selective in the preferential oxidation of carbon monoxide in hydrogen rich stream. Three types of catalysts were prepared by varying the impregnation sequence of Ir or Fe on the alumina support, with the main objective of understanding the role of Fe species during the reaction and revealing the relationship between the catalytic performance and the material structure.

2. Experimental

2.1. Catalyst preparation

$IrFe/Al_2O_3$ was prepared by sequential incipient wetness impregnation. In detail, γ-Al_2O_3 (BET surface area: 230 m^2/g) was first impregnated with an aqueous solution of $Fe(NO_3)_3{\cdot}9H_2O$, followed by drying at 80 °C for 12 h and calcination at 550 °C for 4 h to obtain Fe/Al_2O_3. Then, Ir was deposited on the Fe/Al_2O_3 by the same procedure with $H_2IrCl_6{\cdot}6H_2O$ as a precursor. After being calcined at 320 °C for 5 h, the final catalyst $IrFe/Al_2O_3$ was obtained. By contrast, $FeIr/Al_2O_3$ catalyst was obtained by an inverse impregnation sequence to the above $IrFe/Al_2O_3$ catalyst, while co-$IrFe/Al_2O_3$ was prepared by co-impregnation of γ-Al_2O_3 with the two metal precursors. Ir content in all the catalyst samples was fixed at 1 wt.%, and Fe content was varied to give Fe/Ir atomic ratio of 1/1, 2/1, 5/1, 10/1. For comparison, 1 wt.% Ir/Al_2O_3 and 1 wt.% Ir/Fe_2O_3 were also prepared by impregnation.

2.2. Catalytic activity tests

The catalytic performances for PROX were evaluated using a fixed-bed reactor under atmospheric pressure. Prior to the test, the catalyst sample was in situ reduced with H_2 at 300 °C for 2 h. After cooling to room temperature in He, a reacting gas mixture containing 2% CO, 1% O_2 and 40% H_2 in He was passed through the catalyst bed at a flow rate of 67 cm^3 min^{-1} (STP), corresponding to a space velocity of 40,000 ml/h g-cat. The effluent gas was on-line analyzed by a gas chromatograph (Angilent GC-6890) equipped with a TCD detector.

2.3. Catalyst characterization

Powder X-ray diffraction (XRD) of the samples was performed on a Rigaku (D/MAX-βB) diffractometer equipped with an on-line computer. Diffraction patterns were recorded with Ni-filtered Cu Kα radiation (40 kV, 250 mA) over a 2θ range of 10–80°.

The reducibilities of the calcined catalyst samples were measured by temperature-programmed reduction (TPR) using a Micromeritics AutoChem 2920 apparatus. Prior to the measurement, the catalyst sample was pretreated in Ar at 120 °C for 2 h to remove the adsorbed water. After cooling to room temperature in Ar, the gas flow was switched to 10% H_2 in Ar and the sample was heated from room temperature to 800 °C with a temperature ramp of 10 °C/min. H_2 consumption was determined by TCD.

Absorption FT-IR spectra were collected in single beam mode, with a resolution of 2 cm^{-1}, using a Bruck EQUINOX 55 Spectrometer equipped with a MCT detector cooled by liquid nitrogen. The catalyst sample was pressed into self-supporting wafer and loaded into a quartz IR cell with CaF_2 windows. Prior to CO adsorption, the sample was in situ pre-treated with H_2 at 300 °C for 2 h and then evacuated at 350 °C for 0.5 h. After cooling to room temperature, IR spectrum was recorded as the background. Then, 9 Torr CO was dosed onto the wafer and kept for 10 min, followed by evacuation at room temperature for 0.5 h. The IR spectrum was recorded again. The final spectrum was obtained by subtracting the background from the IR spectrum of CO adsorption.

Microcalorimetric measurements of CO and O_2 adsorption were performed using a BT2.15 heat-flux calorimeter. The calorimeter was connected to a gas handling and a volumetric system employing MKS 698A Baratron Capacitance Manometers for precision pressure measurement ($\pm 1.33 \times 10^{-2}$ Pa) [21]. Prior to the CO or O_2 adsorption, the sample was heated to 300 °C in 30 min and held at this temperature for 2 h in a special treatment cell under a dynamic high pure H_2 (99.999%) atmosphere, followed by evacuation at 350 °C for 1 h. The adsorption experiment was conducted at 40 °C and the detailed procedures for microcalorimetric adsorption have been described earlier [22].

3. Results and discussion

3.1. Effect of Fe content on the catalytic performances

Fig. 1A and B, respectively, illustrate the CO conversions and O_2 selectivities towards CO_2 formation as a function of reaction temperature over a series of $IrFe/Al_2O_3$ catalysts with different Fe/Ir ratios. As references, Ir/Al_2O_3 and Ir/Fe_2O_3 were also investigated. It can be seen that the Ir/Al_2O_3 sample exhibited very poor activity; CO conversion got only 14.8% at 220 °C. This is significantly lower than that on Pt/Al_2O_3 [23]. In contrast, the Ir/Fe_2O_3 manifested a better performance than the Ir/Al_2O_3, with the maximum CO conversion of 47.5% at 160 °C. It was very interesting that when Ir was deposited on Fe-modified Al_2O_3, the catalytic performances were remark-

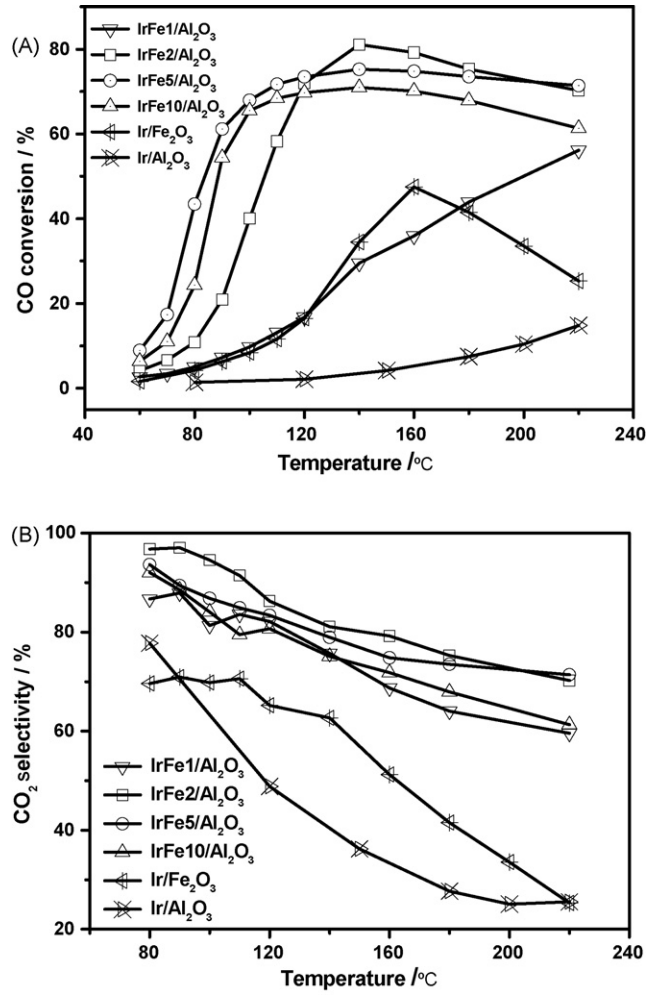

Fig. 1. (A) CO conversions and (B) CO_2 selectivities vs. reaction temperature over $IrFe/Al_2O_3$ catalysts.

ably enhanced. Especially over the $IrFe5/Al_2O_3$, the CO conversion attained 68% at 100 °C, and the oxygen selectivity towards CO_2 formation was 86.8% at this temperature. It can also be seen that there exists an optimum Fe content, that is, Fe/Ir = 5/1. Either a lower (e.g. Fe/Ir = 1 and Fe/Ir = 2) or a higher (e.g. Fe/Ir = 10) Fe content resulted in a decrease in the catalytic activity. Such a difference in catalytic activity with Fe content was particularly remarkable at ∼80 °C, which is important for fuel cell applications. Over all the catalysts investigated, the selectivities of O_2 towards CO oxidation went down with the rising of the reaction temperature due to the competing reaction of H_2 oxidation. However, it is worthwhile to note that the selectivities for CO oxidation over the $IrFe5/Al_2O_3$ catalyst kept a very high value (∼80%) in a wide temperature range (80–200 °C).

To get the structural information on the highly active and selective catalyst $IrFe5/Al_2O_3$, we examined the XRD patterns of the $IrFe/Al_2O_3$ samples with different Fe/Ir ratios. As shown in Fig. 2, only diffraction peaks corresponding to γ-Al_2O_3 were observed on the Ir/Al_2O_3, $IrFe2/Al_2O_3$ and $IrFe5/Al_2O_3$, neither Fe species nor Ir species could be found in the XRD patterns of the above three samples, indicating both Fe species and Ir

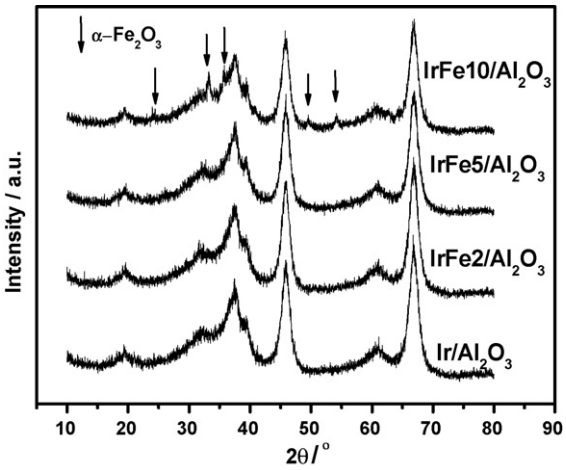

Fig. 2. XRD patterns of calcined $IrFe/Al_2O_3$ catalysts.

species were highly dispersed on the support. Contrary to the above three samples, when Fe/Ir was greater than 5 (for $IrFe10/Al_2O_3$), there appeared very weak peaks corresponding to α-Fe_2O_3 phase [JSPDF00-001-1053], suggesting that the Fe content of the $IrFe10/Al_2O_3$ may be probably over the maximum amount that can be dispersed as a monolayer onto the alumina support [24].

Since the catalytic performances were obtained over the pre-reduced catalysts, it is informative to investigate the reducibilities of the catalysts. Fig. 3 illustrates H_2-TPR profiles of the $IrFe/Al_2O_3$ catalysts with various Fe content. A strong reduction peak occurred at about 130 °C, accompanied with three minor peaks centered at 280–300 °C, 350–400 °C and 450–500 °C, respectively. According to the literature [25], the latter three peaks were due to reduction of Fe_2O_3 to Fe_3O_4, FeO and Fe. With an increase of Fe content, these three peaks shifted to higher temperatures, suggesting that bulk Fe_2O_3 is more difficult to be reduced than the highly dispersed ones. On the other hand, the first strong reduction peak should be mainly caused by the reduction IrO_2 to Ir, together with the partial reduction of Fe_2O_3. Considering the catalytic tests were

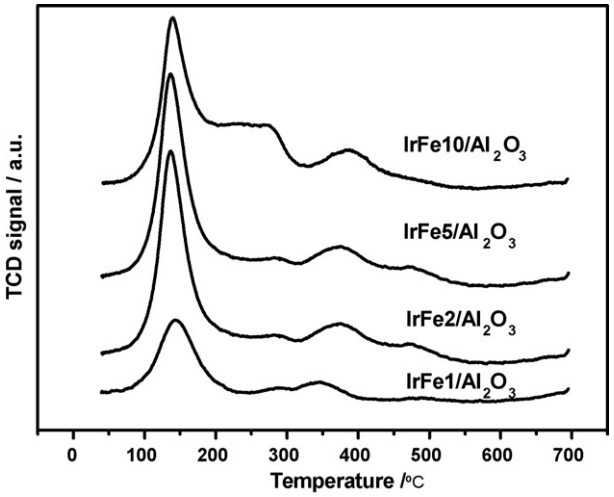

Fig. 3. H_2-TPR profiles of calcined $IrFe/Al_2O_3$ catalysts.

performed after the reduction pretreatment at 300 °C, we can roughly estimate that under this condition, the reduction degree for $Fe^{3+} \rightarrow Fe^{2+}$ was 8%, 42%, 66% and 65% for IrFe1/Al_2O_3, IrFe2/Al_2O_3, IrFe5/Al_2O_3 and IrFe10/Al_2O_3, respectively.

3.2. Effect of impregnation sequence on the catalytic performance

Fig. 4 compares the catalytic performance of IrFe5/Al_2O_3 with those of the other two catalysts: co-IrFe5/Al_2O_3 and Fe5Ir/Al_2O_3. The three catalysts had the same Fe/Ir of 5/1, but they were prepared with different impregnation sequences. The co-IrFe5/Al_2O_3 catalyst was prepared by co-impregnation of γ-Al_2O_3 with the mixture of the two metal precursors, $Fe(NO_3)_3{\cdot}9H_2O$ and $H_2IrCl_6{\cdot}6H_2O$; while the Fe5Ir/Al_2O_3 catalyst was prepared with an inverse impregnation sequence to the IrFe5/Al_2O_3, i.e., impregnating the pre-calcined Ir/Al_2O_3 with $Fe(NO_3)_3{\cdot}9H_2O$. From Fig. 4 we can see that the IrFe5/Al_2O_3 catalyst was the most active and selective one among the three samples, while the Fe5Ir/Al_2O_3 was the poorest catalyst. Obviously, the remarkable difference in their catalytic performances should be caused by the difference in impregnation sequence of Ir and Fe on the Al_2O_3 support.

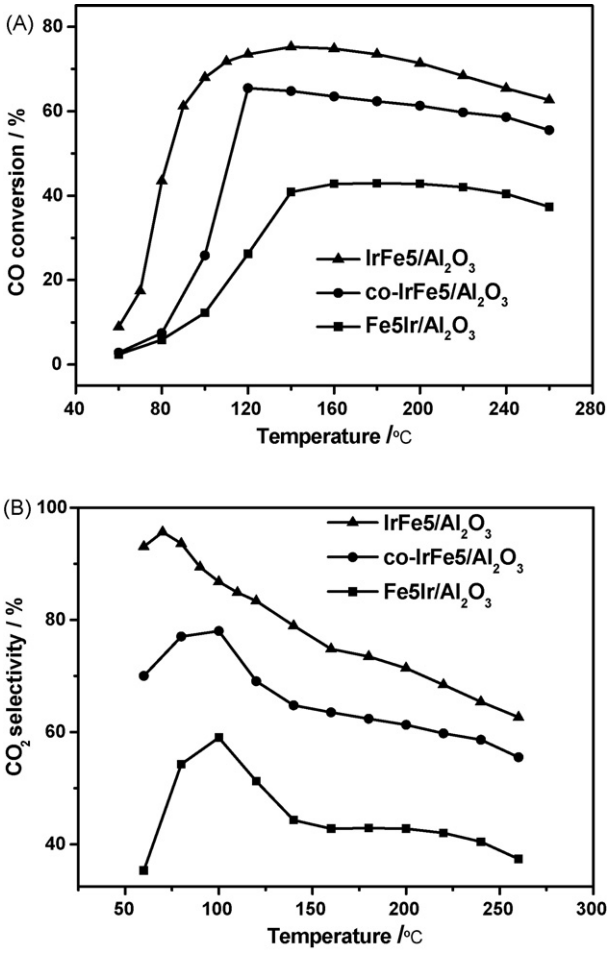

Fig. 4. (A) CO conversions and (B) CO_2 selectivities vs. reaction temperature over FeIr/Al_2O_3, co-IrFe/Al_2O_3 and IrFe/Al_2O_3 catalysts.

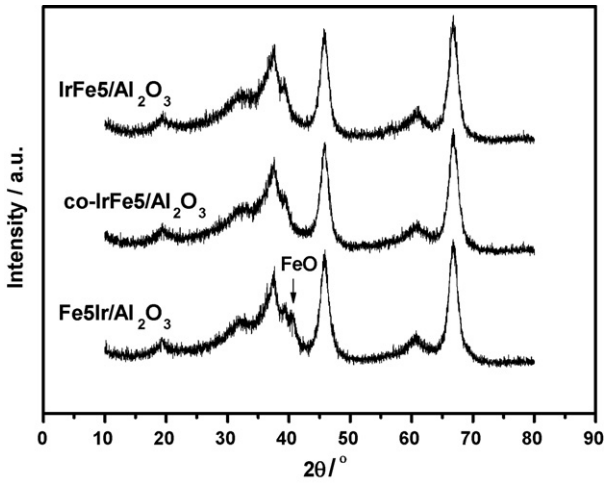

Fig. 5. XRD patterns of FeIr/Al_2O_3, co-IrFe/Al_2O_3 and IrFe/Al_2O_3 catalysts reduced at 300 °C with H_2 for 2 h.

Fig. 5 shows the XRD patterns of IrFe5/Al_2O_3, co-IrFe5/Al_2O_3 and Fe5Ir/Al_2O_3 catalysts. It should be pointed out that the three samples were pre-reduced by H_2 at 300 °C for 2 h before subjected to XRD examinations, and they had the same Ir content and Fe/Ir ratio. Similar to the XRD pattern of the IrFe5/Al_2O_3 shown in Fig. 2, there was no either Ir or FeO_x species which can be detected on the co-IrFe/Al_2O_3 sample, indicating that the two species are highly dispersed on the support. However, for the Fe5Ir/Al_2O_3 catalyst, we observed a very weak peak positioned at 41°, which can be attributed to FeO species [JSPDF00-002-1180]. This result suggests that Ir species are always highly dispersed on the support, irrespective of the impregnation sequence. However, FeO_x species were better dispersed on the pure alumina support than on the Ir/Al_2O_3 support.

Fig. 6 compares the H_2-TPR profiles of IrFe5/Al_2O_3, co-IrFe5/Al_2O_3 and Fe5Ir/Al_2O_3 catalysts. It can be seen that both the position and strength of the first reduction peak on the three samples differs markedly, with the reduction temperature shifting to higher values in the order of: IrFe5/Al_2O_3

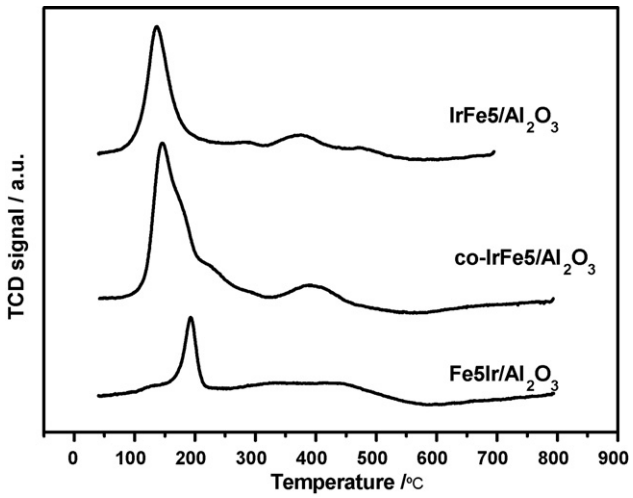

Fig. 6. H_2-TPR profiles of FeIr/Al_2O_3, co-IrFe/Al_2O_3 and IrFe/Al_2O_3 catalysts.

$<$ co-IrFe5/Al_2O_3 $<$ Fe5Ir/Al_2O_3. Since the first peak is mainly caused by the reduction of IrO_2 to Ir, the highest reduction temperature of the Fe5Ir/Al_2O_3 catalyst demonstrated that the deposition of Fe_2O_3 on the Ir/Al_2O_3 made IrO_2 species less reducible. This is probably because IrO_2 species had been covered by its upper FeO_x layer. On the contrary, for the IrFe/Al_2O_3 sample, since most IrO_2 species was exposed on the Fe-modified support, it can be easily reduced together with the partial reduction of Fe_2O_3. For the co-IrFe/Al_2O_3 sample, both Ir and Fe species were simultaneously impregnated onto the Al_2O_3 support so that they were equally exposed to H_2 and were reduced to a larger extent. Actually, the reduction degree at 300 °C for $Fe^{3+} \rightarrow Fe^{2+}$ on the sample co-IrFe5/Al_2O_3 was estimated to be over 100%, suggesting that a part of Fe^{3+} was further reduced to Fe^0. Meanwhile, we cannot yet exclude the possibility that a minor part of IrO_2 particles were buried into FeO_x, which led to the reduction peak shifting to a higher temperature.

3.3. Reaction mechanism implicated by FT-IR and microcalorimetry

In order to make it clear what sites on the catalyst the reactant molecules were adsorbed, we investigated CO and O_2 adsorption on the catalyst surface by means of FT-IR and microcalorimetry.

Fig. 7 illustrates the FT-IR spectra of CO adsorption on the different catalysts. The bands at 2076, 2049 and 2003 cm^{-1} can be assigned to CO linearly adsorbed on different Ir^0 sites [26,27], while the bands at 1658, 1437 and 1229 cm^{-1} are due to the formation of CO_3^{2-} upon CO adsorption on the Al_2O_3 support [28]. Clearly, the strongest absorption bands due to CO adsorption on Ir^0 appeared on the IrFe/Al_2O_3, which are even stronger than those on the Ir/Al_2O_3. This indicates that FeO_x species on the alumina support promotes the CO adsorption on the Ir^0 sites via interacting with Ir species. By contrast, the CO adsorption on the co-IrFe/Al_2O_3 and FeIr/Al_2O_3 catalysts was comparatively weak, probably caused by the covering of

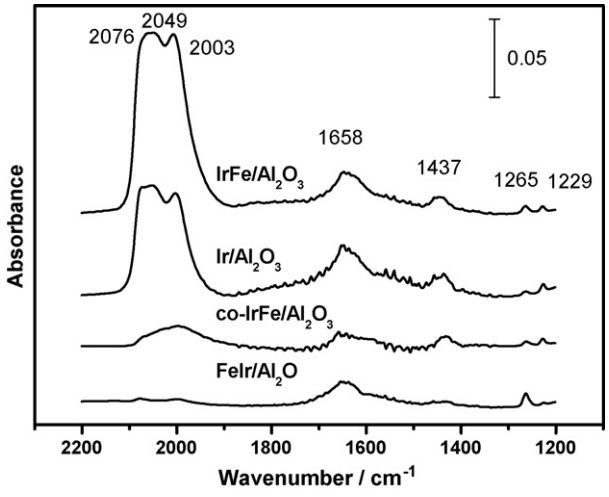

Fig. 7. In situ FT-IR spectra of CO adsorbed on FeIr/Al_2O_3, co-IrFe/Al_2O_3 and IrFe/Al_2O_3 catalysts at room temperature.

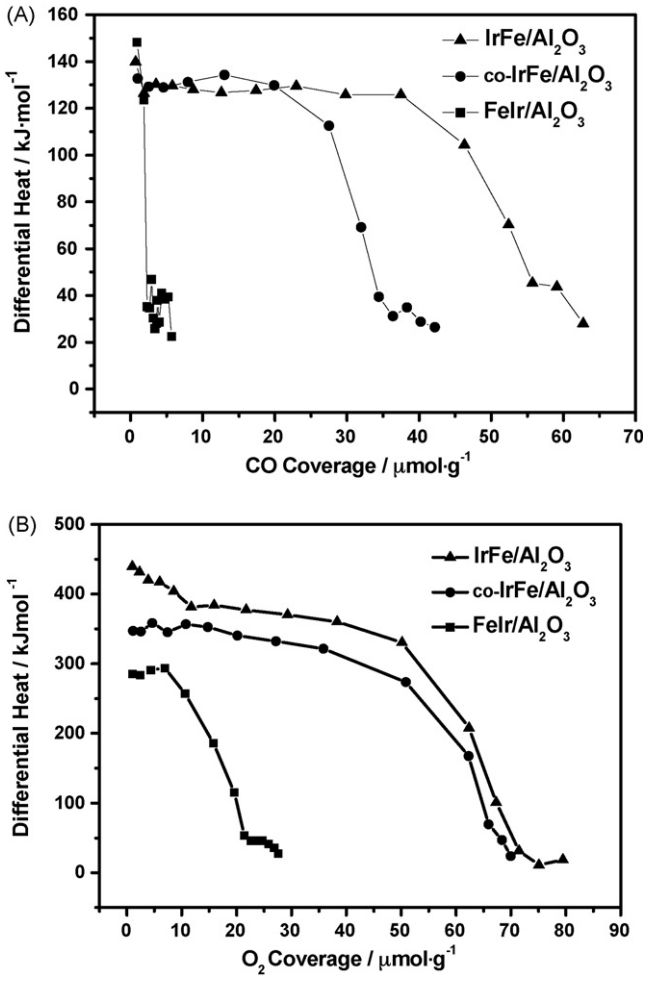

Fig. 8. Differential heat curve vs. coverage of CO (A) and O_2 (B) adsorption on fresh catalysts by microcalorimetry.

Ir active sites with FeO_x species. This is in agreement with the TPR results in Section 3.2.

To further confirm this result, a more quantitative technique, microcalorimetry, was employed to precisely measure the amount of CO or O_2 adsorbed on the catalyst surface, as well as the adsorption heat. Fig. 8 shows the differential heat as a function of coverage of O_2 and CO adsorbed on the three catalysts. The initial adsorption heat and the whole heat flat of O_2 on the catalysts decreased following the order of FeIr/Al_2O_3 $<$ co-IrFe/Al_2O_3 $<$ IrFe/Al_2O_3, indicating the adsorption of O_2 on the IrFe/Al_2O_3 was the strongest. By contrast, in the case of CO adsorption, the initial adsorption heat on the three catalysts was the same within the experimental error, indicating the same sites for CO adsorption existing on the three catalysts. However, the number of sites varied greatly with the different catalysts. Table 1 lists the saturation uptakes of CO and O_2 on the three catalysts. It can be seen that the saturation uptakes of CO on the IrFe/Al_2O_3, co-IrFe/Al_2O_3 and FeIr/Al_2O_3 were 55, 35 and 3.6 μmol/g-cat, respectively, presenting again that the IrFe/Al_2O_3 catalyst had the most Ir sites for CO adsorption while the FeIr/Al_2O_3 had the least. On the other hand, for the O_2 adsorption, the saturation uptakes on the above three catalysts were 63, 62, and 24 μmol/g-cat, respectively.

Table 1
The saturation uptakes of CO and O_2 on fresh catalysts (μmol g^{-1}-cat)

Absorbate	IrFe5/Al_2O_3	co-IrFe/Al_2O_3	Fe5Ir/Al_2O_3
CO	55	35	3.6
O_2	63	62	24

This trend was slightly different from the case of CO adsorption, since both Ir sites and FeO_x sites can adsorb O_2 molecules.

It has been reported that the presence of transition metal oxides was beneficial to the improvement of alumina (or SiO_2, Carbon, etc.) supported Pt or Au catalysts for PROX [12–20,29–32]. Kotobuki et al. [14] found that Pt-Fe/mordenite exhibited remarkable PROX activity up to an extremely high space velocity. Based on chemisorption measurements, they proposed a ''bifunctional mechanism'' where the Pt sites act for CO adsorption and Fe sites act for O_2 dissociative adsorption, and the reaction between the adsorbed CO and O takes place on the Pt-Fe neighboring sites. Such a non-competitive mechanism for CO oxidation was also suggested by Liu et al. [15] when they investigated an Fe-oxide promoted Pt/Al_2O_3 catalyst. On the other hand, Schubert et al. observed a superior activity of carbon supported Pt-Sn bimetallic catalyst to a commercial Pt/Al_2O_3 system [19]. Their characterization data also supported the above bifunctional mechanism, with competing CO and H_2 adsorption on Pt sites/areas and O_2 adsorption predominantly on Sn/SnO_x islands on or adjacent to the active Pt sites/areas. The reaction takes place at the perimeter of these islands or by invoking a spill-over process.

An important feature of these above-mentioned work is that the amount of promoter, either Fe or Sn, was well below that of Pt. Hence, although Pt was deposited prior to the Fe on the support, only partial coverage of Pt surface by FeO_x occurred. However, for our IrFe/Al_2O_3 catalyst, the optimum Fe/Ir ratio was 5/1. When Fe was deposited prior to Ir on the Al_2O_3 support, Fe_2O_3 was highly dispersed onto the support, probably as a monolayer covering the alumina support, as indicated by the XRD results. Thus, when Ir was deposited on the pre-formed Fe/Al_2O_3, the Ir particles must be highly dispersed on the Fe_2O_3 layer, not on the Al_2O_3 support. Such an impregnation sequence warranted the intimate contact between Ir and Fe, meanwhile maintaining the active Ir exposed to surface for CO adsorption. Contrary to the case of IrFe/Al_2O_3, the structure of FeIr/Al_2O_3 was characterized by the almost full coverage of Ir with the Fe_2O_3, thus CO adsorption on the Ir sites was inhibited by the upper layer Fe_2O_3. Both the IR and microcalorimetry confirmed this structure. On the other hand, when co-impregnation was employed, the resulting co-IrFe/Al_2O_3 presented a structure between the IrFe/Al_2O_3 and FeIr/Al_2O_3. That is, only partial coverage of Ir by Fe_2O_3 occurred, and a part of Ir active sites were exposed on the surface of Fe/Al_2O_3 or pure Al_2O_3 support.

From the above discussions, it is understandable that the activity difference between the three catalysts is determined by their different structures. As proposed in the literature [14,15,19], a similar bifunctional mechanism probably works in our IrFe/Al_2O_3 catalyst. CO was adsorbed on metallic Ir sites and O_2 was adsorbed on the FeO_x sites; the reaction took place at the interface between Ir and FeO_x or via a spill-over process, thus eliminating the inhibiting effect of CO adsorption on the monometallic Ir catalysts. The high activity of the IrFe/Al_2O_3 should be attributed to its good ability for both O_2 and CO adsorption, whereas the poor behavior of FeIr/Al_2O_3 towards CO adsorption can account for its poor activity. However, it should be pointed out that some type of interaction might exist between the Fe_2O_3 and Ir, as indicated by the simultaneous reduction of IrO_2 and Fe_2O_3 and by the stronger adsorption of CO on the IrFe/Al_2O_3 than on the Ir/Al_2O_3.

4. Conclusions

In this work, we designed a novel bifunctional catalyst IrFe/Al_2O_3 with high activity and selectivity for PROX. Three catalysts with different structures have been prepared by varying the impregnation sequence. Among them, IrFe/Al_2O_3 catalyst with the Fe/Ir ratio of 5/1 exhibited the best catalytic performance. A combination of characterization techniques were employed to reveal the relationship between the catalytic performance and the structure. When Ir was deposited on the underlying Fe_2O_3 layer, the resulting catalyst can strongly adsorb both O_2 and CO, leading to an enhanced activity for CO oxidation. On the contrary, when most Ir sites were covered by the upper Fe_2O_3 layer, CO adsorption on the Ir sites was greatly inhibited and the catalytic activity was very low. Similar to the Fe promoted Pt-based catalysts, the IrFe/Al_2O_3 also served as a bifunctional catalyst for PROX reaction.

Acknowledgement

Support of National Science Foundation of China (NSFC) for Distinguished Young Scholars (No. 20325620) is gratefully acknowledged.

References

[1] C. Song, Catal. Today 77 (2002) 17.
[2] B. Smitha, S. Sridhar, A.A. Khan, J. Membr. Sci. 259 (2001) 10.
[3] C.D. Dudfield, R. Chen, P.L. Adcock, J. Power Sources 86 (2000) 214.
[4] T.V. Choudhary, D.W. Goodman, Catal. Today 77 (2002) 65.
[5] D.L. Trimm, Z.I. Onsan, Catal. Rev. 43 (2001) 31.
[6] D.L. Trimm, Appl. Catal. A 96 (2005) 1.
[7] W.B. Kim, T. Voitl, G.J. Rodriguez-Rivera, S.T. Evans, J.A. Dumesic, Angew. Chem. Int. Ed. 44 (2005) 778.
[8] M. Okumura, N. Masuyama, E. Konishi, S. Ichikawa, T. Akita, J. Catal. 208 (2002) 485.
[9] F. Mariño, C. Descorme, D. Duprez, Appl. Catal. B 54 (2004) 59.
[10] R.J.H. Grisel, B.E. Nieuwenhuys, J. Catal. 199 (2001) 48.
[11] S.Y. Chin, O.S. Aleseev, M.D. Amiridis, J. Catal. 243 (2006) 329.
[12] A. Sirijaruphan, J.G. Goodwin, R.W. Rice, J. Catal. 224 (2004) 304.
[13] M. Watanabe, H. Uchida, K. Ohkubo, H. Igarashi, Appl. Catal. B 46 (2003) 595.
[14] M. Kotobuki, A. Watanabe, H. Uchida, H. Yamashita, M. Watanabe, J. Catal. 236 (2005) 262.
[15] X.S. Liu, O. Korotkikh, R. Farrauto, Appl. Catal. A 226 (2002) 293.
[16] C. Kwak, T.J. Park, D.J. Suh, Appl. Catal. A 278 (2005) 181.
[17] S. Özkara, A.E. Aksoylu, Appl. Catal. A 251 (2003) 75.

[18] E. Simsek, S. Özkara, A.E. Aksoylu, Z.I. Önsan, Appl. Catal. A 316 (2007) 169.
[19] M.M. Schubert, M.J. Kahlich, G. Feldmeyer, M. Huttner, S. Hackenberg, H.A. Gasteiger, R.J. Behm, Phys. Chem. Chem. Phys. 3 (2001) 1123.
[20] E.Y. Ko, E.D. Park, K.W. Seo, H.C. Lee, D. Lee, S. Kim, Catal. Lett. 110 (2006) 275.
[21] L. Li, X. Wang, J. Shen, L. Zhou, T. Zhang, J. Therm. Anal. Calorim. 82 (2005) 103.
[22] L. Li, X.D. Wang, J.Y. Shen, L.X. Zhou, T. Zhang, Chin. J. Catal. 24 (2003) 872.
[23] S.H. Oh, R.M. Sinkevitch, J. Catal. 142 (1993) 254.
[24] Y.C. Xie, Y.Q. Tang, Adv. Catal. 37 (1990) 1.
[25] P. Reyes, H. Rojas, J.L.G. Fierro, J. Mol. Catal. A 203 (2003) 203.
[26] F. Solymosi, E. Novak, A. Molnar, J. Phys. Chem. 94 (1990) 7250.
[27] F. Solymosi, J. Rasko, J. Catal. 62 (1980) 253.
[28] J. Baltrusaitis, J.H. Jensen, V.H. Grassian, J. Phys. Chem. B 110 (2006) 12005.
[29] J.L. Ayastuy, M.P. González-Marcos, J.R. González-Velasco, M.A. Gutiérrez-Ortiz, Appl. Catal. B 70 (2007) 532.
[30] M.M. Schubert, S. Hackenberg, A.C.V. Veen, M. Muhler, V. Plzak, R.J. Behm, J. Catal. 197 (2001) 113.
[31] D.A. Bulushev, L. Kiwi-Minsker, I. Yuranov, E.I. Suvorova, P.A. Buffat, A. Renken, J. Catal. 210 (2002) 149.
[32] D.H. Wang, Z.P. Hao, D.Y. Cheng, X.C. Shi, C. Hu, J. Mol. Catal. A 200 (2003) 229.